Acta Crystallographica Section B
**Structural Science**
ISSN 0108-7681

# Polymorphism in iodotris(tri-*p*-tolylphosphine)silver(I)

**Gertruida J. S. Venter,[a] Andreas Roodt[a] and Reinout Meijboom[b]***

[a]Department of Chemistry, University of the Free State, PO Box 339, Bloemfontein, South Africa, and [b]Department of Chemistry, University of Johannesburg, PO Box 524, Auckland Park, 2006 Johannesburg, South Africa

Correspondence e-mail: rmeijboom@uj.ac.za

Received 25 August 2008
Accepted 12 January 2009

The reaction of silver(I) iodide with tri(*p*-tolyl)phosphine in MeCN solution in 1:3 molar ratio yields a polymorph of the complex of the formula [AgI{P(4-MeC$_6$H$_4$)$_3$}$_3$], with the Ag atom in a distorted tetrahedral environment. A polymorphic structure of this complex (*a*) is compared with previously published crystal structures (*b*), determined at different temperatures. The two polymorphs are compared using r.m.s. overlay calculations as well as half-normal probability plots.

## 1. Introduction

The first silver phosphine complex, [AgPPr$_3$]SCN, characterized by X-ray crystallography was reported in 1963 (Panattoni & Frasson, 1963). Since then more than a thousand (Cambridge Structural Database, CSD; Allen, 2002) complexes containing silver coordinated to phosphorous donor ligands have been synthesized and characterized. In the past it was shown that silver(I) complexes can crystallize in different polymorphic variations, leading to such extreme differences as 'cubic' (Teo & Calabrese, 1976*a*) and 'step' tetramers, depending on the solvent of crystallization (Teo & Calabrese, 1976*b*). We recently reviewed the structural chemistry of silver(I) complexes with, mainly, phosphine ligands (Meijboom *et al.*, 2009) and refer to this review for more information on the various complexes. An interest in the ability of silver(I) complexes to adopt geometries with variable nuclearities has led to the study of silver(I) complexes with various counterions and different ratios of tri(*p*-tolyl)-phosphine (Meijboom *et al.*, 2006; Meijboom, 2006; Meijboom & Muller, 2006; Venter *et al.*, 2006, 2007). This paper reports a polymorph of [AgI{P(4-MeC$_6$H$_4$)$_3$}$_3$] (1), in monoclinic space group *C*2/*c* (*a*). This polymorph is compared with the polymorph in triclinic space group $P\bar{1}$ (*b*). We communicated polymorph (*b*), collected at 293 K, previously (Meijboom, 2007). Subsequently a report appeared containing a re-determination of polymorph (*b*) at 293 K as well as at 140 K (Zartilas *et al.*, 2007). Here we present a description of the two polymorphs. The differences in geometry between the two polymorphs are described by r.m.s. overlay calculations and analysed by half-normal probability plot analysis.

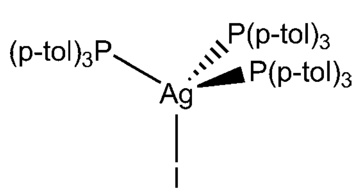


**(1)**

**Table 1**
Crystal data and structural refinement for (1).

| | |
|---|---|
| Crystal data | |
| Chemical formula | $C_{63}H_{63}AgIP_3$ |
| $M_r$ | 1147.82 |
| Cell setting, space group | Monoclinic, $C2/c$ |
| Temperature (K) | 100 (2) |
| $a$, $b$, $c$ (Å) | 22.745 (3), 11.0100 (12), 44.797 (5) |
| $\beta$ (°) | 103.007 (5) |
| $V$ (Å$^3$) | 10930 (2) |
| $Z$ | 8 |
| $D_x$ (Mg m$^{-3}$) | 1.395 |
| Radiation type | Mo $K\alpha$ |
| $\mu$ (mm$^{-1}$) | 1.06 |
| Crystal form, colour | Cuboid, colourless |
| Crystal size (mm) | 0.26 × 0.2 × 0.17 |
| | |
| Data collection | |
| Diffractometer | CCD area detector |
| Data collection method | $\varphi$ and $\omega$ scans |
| Absorption correction | Multi-scan (based on symmetry-related measurements) |
| $T_{min}$ | 0.770 |
| $T_{max}$ | 0.840 |
| No. of measured, independent and observed reflections | 88 005, 13 655, 12 118 |
| Criterion for observed reflections | $I > 2\sigma(I)$ |
| $R_{int}$ | 0.033 |
| $\theta_{max}$ (°) | 28.4 |
| | |
| Refinement | |
| Refinement on | $F^2$ |
| $R[F^2 > 2\sigma(F^2)]$, $wR(F^2)$, $S$ | 0.026, 0.058, 1.07 |
| No. of reflections | 13 655 |
| No. of parameters | 623 |
| H-atom treatment | Constrained† |
| Weighting scheme | $w = 1/[\sigma^2(F_o^2) + (0.0182P)^2 + 18.1054P]$, where $P = (F_o^2 + 2F_c^2)/3$ |
| $(\Delta/\sigma)_{max}$ | 0.004 |
| $\Delta\rho_{max}$, $\Delta\rho_{min}$ (e Å$^{-3}$) | 0.43, −0.50 |
| Extinction method | *SHELXL* |
| Extinction coefficient | 0.000064 (7) |

Computer programs used: *APEX*2 (Bruker, 2005), *SAINT-Plus* (Bruker, 2004*a*), *SHELXS*97 and *SHELXL*97 (Sheldrick, 2008), *DIAMOND*3.0c (Brandenburg & Putz, 2005), *WinGX* (Farrugia, 1999). † Constrained to parent site.

**Table 2**
Selected interatomic bond distances (Å) and angles (°) for (1).

| | $a$, 100 K[a] | $b$, 293 K[b] | $b$, 140 K[c] | $b$, 293 K[c] |
|---|---|---|---|---|
| Ag1—I1 | 2.838 (1) | 2.8683 (5) | 2.8737 (7) | 2.8655 (9) |
| Ag1—P1 | 2.5052 (7) | 2.5346 (9) | 2.521 (2) | 2.529 (2) |
| Ag1—P2 | 2.5088 (6) | 2.5562 (9) | 2.545 (2) | 2.553 (2) |
| Ag1—P3 | 2.5238 (5) | 2.5617 (9) | 2.545 (1) | 2.559 (2) |
| I1—Ag1—P1 | 103.85 (2) | 102.35 (2) | 101.55 (4) | 102.37 (5) |
| I1—Ag1—P2 | 101.37 (2) | 99.38 (2) | 98.57 (3) | 99.44 (5) |
| I1—Ag1—P3 | 111.84 (2) | 111.51 (2) | 112.12 (4) | 111.54 (5) |
| P1—Ag1—P2 | 111.46 (2) | 112.04 (3) | 112.31 (5) | 111.94 (6) |
| P1—Ag1—P3 | 114.41 (2) | 117.65 (3) | 118.13 (5) | 117.81 (6) |
| P2—Ag1—P3 | 112.78 (2) | 111.94 (3) | 111.87 (5) | 111.77 (6) |
| $d$(Ag1—PPP plane) | 0.6838 (4) | 0.6421 (3) | 0.6259 (5) | 0.6429 (8) |

References: (*a*) this work, (*b*) Meijboom (2007), (*c*) Zartilas *et al.* (2007).

## 2. Experimental

### 2.1. Synthesis

The title complex, [AgI{P(4-MeC$_6$H$_4$)$_3$}$_3$] (1), was prepared by adding AgI (0.1023 g, 0.437 mmol) to a solution of P(4-MeC$_6$H$_4$)$_3$ (0.3977 g, 1.31 mmol) in acetonitrile (10 ml). The resulting solution was subsequently heated under reflux for 30 min. Crystallization produced colourless crystals, suitable for X-ray diffraction (0.4943 g, 98.7%). Spectroscopic data were identical to data previously reported (Zartilas *et al.*, 2007).

### 2.2. Crystallography and calculations

Crystals of (1) were grown from acetonitrile at room temperature. Single-crystal X-ray diffraction data for (1) were collected on a Bruker X8 Apex II 4 K Kappa CCD diffractometer using Mo $K\alpha$ (0.71073 Å) radiation with $\varphi$ and $\omega$ scans at 100 (2) K. The initial unit cell and data collection were achieved by the *APEX*2 (Bruker, 2005) software utilizing *COSMO* (Bruker, 2003) for optimum collection of the reciprocal space. All reflections were merged and integrated using *SAINT* (Bruker, 2004*a*) and were corrected for Lorentz, polarization and absorption effects using *SADABS* (Bruker, 2004*b*). The structures were solved by the direct method using *SIR*97 (Altomare *et al.*, 1999) and refined through full-matrix least-squares cycles using the *SHELXL*97 (Sheldrick, 2008) software package with $\Sigma(|F_o| - |F_c|)^2$ being minimized. All non-H atoms were refined with anisotropic displacement parameters.

Aromatic and methyl H atoms were placed in geometrically idealized positions (C—H = 0.95 Å for aromatic and 0.98 Å for Me) and constrained to ride on their parent atoms, with $U_{iso}(H) = 1.2U_{eq}(C)$ for aromatic and $1.5U_{eq}(C)$ for methyl H atoms. The deepest residual electron-density hole (−0.50 e Å$^{-3}$) is located 1.48 Å from H125, and the highest peak (0.43 e Å$^{-3}$) 0.86 Å from H22C. Crystal data and details of data collection and refinement are given in Table 1.[1]

All structures were checked for solvent accessible cavities using *PLATON* (Spek, 1990) and the graphics were performed with the *DIAMOND* (Brandenburg & Putz, 2005) Visual Crystal Structure Information System software. The r.m.s. calculations were performed with *HyperChem* (Hypercube, 2002). Data for the half-normal probability plots were processed using *EXCEL*2003 (Microsoft, 2003).

## 3. Results and discussion

Three coordinate complexes of the type [Ag(P$R_3$)$_3$]$^+$ are exceedingly rare and require a non-coordinating anion to form (Meijboom *et al.*, 2009). In addition, only a few tetrahedral complexes of the type [Ag$X${$ZR_3$}$_3$] [$X$ = Cl, Br, I; $ZR_3$ = PPh$_3$ (Engelhardt *et al.*, 1987; Camalli & Caruso, 1987; Hibbs *et al.*, 1996), AsPh$_3$ (Pelizzi *et al.*, 1985; Bowmaker *et al.*, 1997); $X$ = Cl, I; $ZR_3$ = SbPh$_3$ (Effendy *et al.*, 1997)] have been structurally characterized. The X-ray structure determination of compound (1) shows the expected monomeric [AgI{P(4-MeC$_6$H$_4$)$_3$}$_3$] with a distorted tetrahedral geometry around the

[1] Supplementary data for this paper are available from the IUCr electronic archives (Reference: BP5016). Services for accessing these data are described at the back of the journal.

**Table 3**
Comparison of structural parameters (Å, °) in related [Ag$X${P(4-MeC$_6$H$_4$)$_3$}$_3$] compounds.

| $X$ | I[a] | Cl[b] | Br[b] | SCN[c] |
|---|---|---|---|---|
| Ag—$X$ | 2.838 (1) | 2.6186 (17) | 2.7050 (6) | 2.6617 (7) |
| Ag—P1 | 2.5052 (7) | 2.5347 (11) | 2.5545 (10) | 2.5288 (5) |
| Ag—P2 | 2.5088 (6) | 2.5566 (12) | 2.5367 (10) | 2.5329 (6) |
| Ag—P3 | 2.5238 (5) | 2.5609 (11) | 2.5624 (10) | 2.5505 (6) |
| $X$—Ag—P1 | 103.85 (2) | 108.88 (5) | 109.39 (3) | 110.75 (2) |
| $X$—Ag—P2 | 101.37 (2) | 104.17 (5) | 103.66 (3) | 104.23 (2) |
| $X$—Ag—P3 | 111.84 (2) | 99.54 (5) | 99.95 (3) | 95.83 (2) |
| P1—Ag1—P2 | 111.46 (2) | 115.89 (4) | 115.92 (4) | 116.18 (2) |
| P1—Ag1—P3 | 114.41 (2) | 108.40 (4) | 108.06 (3) | 108.20 (2) |
| P2—Ag1—P3 | 112.78 (2) | 118.22 (4) | 118.25 (3) | 119.41 (2) |

References: (*a*) this work, (*b*) Zartilas *et al.* (2007), (*c*) Venter *et al.* (2008).

metal ion, formed by the iodide and three phosphorus atoms from the tri-*p*-tolylphosphine ligands. A molecular diagram showing the numbering scheme of the title compound [AgI{P(4-MeC$_6$H$_4$)$_3$}$_3$] (1), polymorph *a*, is presented in Fig. 1, with selected bond lengths and angles in Table 2, including the comparison with the previously reported polymorph *b*. Comparative bond distances and angles for selected related compounds are given in Table 3. The current polymorph crystallizes in the monoclinic space group *C*2/*c* with *Z* = 8.

The angles between the Ag atom and the surrounding atoms vary between 101.37 (2) and 114.41 (2)° and are comparable to previously reported data (Table 2). The Ag—P bond lengths vary from 2.5052 (7) to 2.5238 (5) Å (average distance 2.51 Å) and are shorter than those of polymorph *b* (average distance 2.55 Å). The Ag—I bond distance in polymorph *a* is 2.838 (1) Å, which is shorter than the average Ag—I distance of 2.87 Å in polymorph *b*. The Ag atom is displaced by 0.6838 (4) Å from a plane constructed through the three P atoms, indicating a strong interaction between the Ag and I atoms. Comparison with previously reported [Ag$X${P(4-MeC$_6$H$_4$)$_3$}$_3$] compounds [$X$ = Cl, Br (Zartilas *et al.*, 2007), SCN (Venter *et al.*, 2008); Table 3] shows that roughly the same, tetrahedral, geometry around the Ag atom is present with comparable distances and angles.

The unit cell of polymorph *a* is of such a nature that it could possibly be mistaken for a supercell of polymorph *b*, with both the *a* and the *c* axis in polymorph **a** being about twice as long as that for polymorph *b*. However, the angles of the unit cell are vastly different (Table 4). The difference is also accentuated by the packing of the molecules, which displays four molecules in one half of the unit cell angled in one direction, and the four molecules in the other half orientated in the opposite direction (Fig. 2*a*). The unit cell of polymorph *b* displays two molecules angled in opposite directions (Fig. 2*b*).

Initial inspection of Table 4 would suggest the possibility of different polymorphs for the three collections of polymorph *b* – possibly due to initial solvate inclusion. An elongation of the *c* axis is observed at 293 K (from 22.9 to 23.2 Å), as well as an increase in the cell volume (from 2729 Å$^3$ to an average value of 2799 Å$^3$). The calculated densities of the current polymorph, *a*, and the determination of polymorph *b* at 140 K agree fairly well and indicate an equally effective packing. In addition, the volume of polymorph *a* per molecule corre-

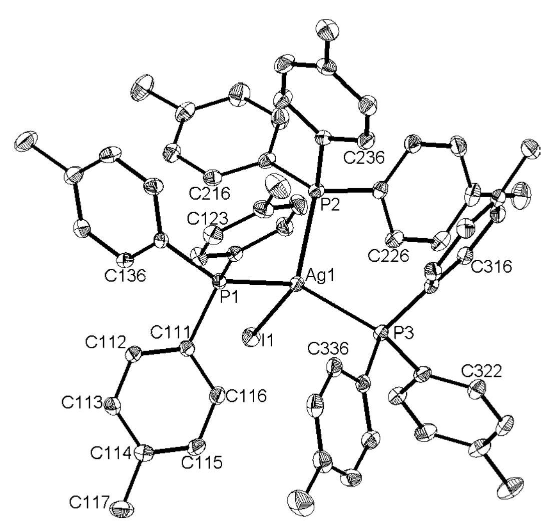


**Figure 1**
Molecular diagram of compound (1), polymorph *a* (50% probability displacement ellipsoids). H atoms are omitted for clarity. For the C atoms, the first digit indicates the phosphine number, the second digit indicates the ring number and the third digit indicates the position of the atom in the ring. Some labels have been omitted for clarity, but all rings are numbered in the same consistent way.

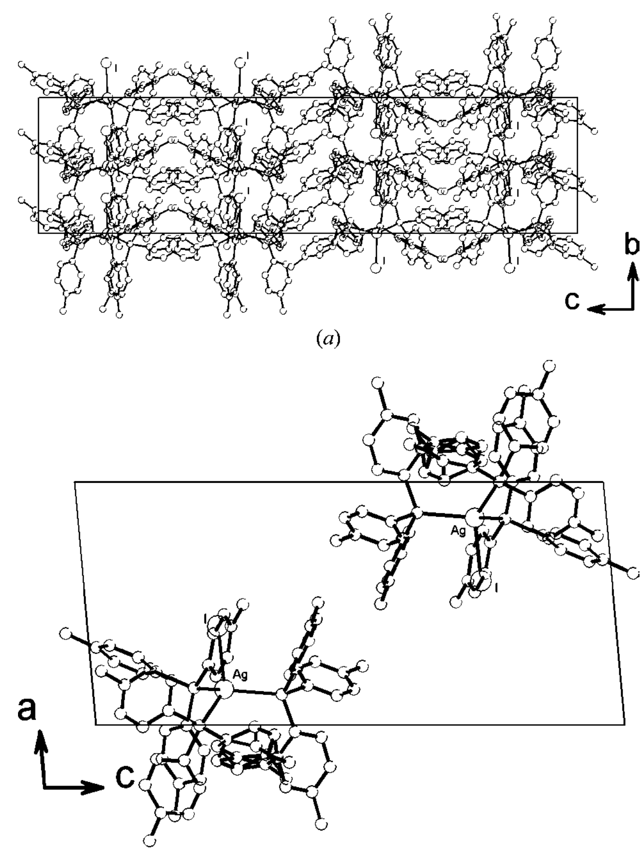


**Figure 2**
(*a*) Packing of *a* in the monoclinic *C*2/*c* unit cell, viewed along the *a* axis, and (*b*) packing of *b* in the triclinic $P\bar{1}$ unit cell, viewed along the *b* axis.

**Table 4**
Comparative crystal data for polymorphs *a* and *b*.

| | *a*; 100 K[a] | *b*; 293 K[b] | *b*; 140 K[c] | *b*; 293 K[c] |
|---|---|---|---|---|
| Temperature (K) | 100 (2) | 293 (2) | 140 (2) | 293 (2) |
| Crystal system | Monoclinic | Triclinic | Triclinic | Triclinic |
| Space group | $C2/c$ | $P\bar{1}$ | $P\bar{1}$ | $P\bar{1}$ |
| $a$ (Å) | 22.745 (3) | 11.043 (1) | 11.008 (5) | 11.038 (2) |
| $b$ (Å) | 11.010 (1) | 11.567 (1) | 11.4509 (5) | 11.548 (2) |
| $c$ (Å) | 44.797 (5) | 23.243 (3) | 22.9459 (8) | 23.227 (5) |
| $\alpha$ (°) | 90 | 99.292 (3) | 99.461 (3) | 99.29 (3) |
| $\beta$ (°) | 103.007 (5) | 92.174 (2) | 91.648 (3) | 92.12 (3) |
| $\gamma$ (°) | 90 | 106.196 (2) | 106.350 (4) | 106.19 (3) |
| $V$ (Å$^3$) | 10930 (2) | 2802.7 (6) | 2728.5 (2) | 2795.2 (11) |
| $Z$ | 8 | 2 | 2 | 2 |
| $\rho_{calc}$ (g cm$^{-3}$) | 1.395 | 1.36 | 1.396 | 1.362 |

References: (*a*) this work, (*b*) Meijboom (2007), (*c*) Zartilas *et al.* (2007).

sponds to 1366 Å$^3$, whereas the volume per molecule, for polymorph *b* corresponds to 1364 (140 K), 1398 [293 K (Zartilas *et al.*, 2007)] and 1401 Å$^3$ [293 K (Meijboom, 2007)]. An increase of $\sim$ 75 Å$^3$ in the volume of the unit cell leaves enough space for a solvent molecule such as acetonitrile. In addition, several structures of silver(I) complexes have been determined containing solvate molecules (Meijboom *et al.*, 2009).

Comparing the cavities in the structures (Spek, 1990) revealed that a general compression (radius decreased 0.06 Å on average) of the cavities occurred when cooling down from 293 to 140 K [for the structures reported (Zartilas *et al.*, 2007)]. The same cavities were observed in the structure reported by us (Meijboom, 2007), but additional cavities on the corners of the unit cell were also observed (see the supplementary information for diagrams) – these cavities were presumably compressed in the other structures to below the detection limit. In addition, the simulated powder pattern (see supplementary information) of the three different reports on polymorph *b* shows an identical pattern, confirming that, despite the rather large differences in cell volume, the compounds are of the same polymorph. The simulated powder pattern of polymorph *a* is significantly different from that of polymorph *b*.

Only one intermolecular interaction (Spek, 1990) is observed in the current polymorph.[2] In contrast, no intermolecular interactions were observed in polymorph *b* as reported by us previously.

The degree of similarity/dissimilarity between two crystalline structures is an important aspect of many investigations in crystallography, chemistry, physics and materials science. Several techniques have been developed in the recent past to describe and calculate this type of similarities. The use of powder diffraction patterns to compare crystal structures have been reported (Karfunkel *et al.*, 1993; De Gelder *et al.*, 2001), however, this provides a global description of the similarities between two structures. The use of radial distribution function (Willighagen *et al.*, 2005) suffers from the same drawback that the exact differences between two structures cannot be easily identified.

A r.m.s. calculation is one way to compare similar structures. For completeness we used all non-H atoms in the molecules for the r.m.s. calculations. The minor component in polymorph *b* was excluded from the r.m.s. calculations. The calculated r.m.s. deviations between the various determinations of polymorph *b* are: $4.27 \times 10^{-2}$ Å for the two determinations at 293 K and 0.293 Å for the 140 K compared with our 293 K determination. These small r.m.s. errors again confirm that these three determinations are of the same polymorph. The r.m.s. error between polymorph *a* and polymorph *b*, as determined at 140 K, however, gives a value of 2.98 Å. In addition, the differences between the two polymorphs can be seen from the overlay of these two structures (Fig. 3). It is clear from Fig. 3 that rotation around some of the P—C bonds result in a different orientation of the *p*-tolyl groups in the two polymorphs. A disorder can be observed in polymorph *b* which stays virtually the same as the temperature decreases. At 293 K, the occupancy of the C atoms on the disordered ring is 0.65 (Meijboom, 2007; 0.64 in Zartilas *et al.*, 2007) and at 140 K the disorder is 0.69.

Ordered weighted differences between matching parameters in independently determined structures follow a Gaussian distribution only if both determinations are subject to the influence of random effects. Departures from Gaussian are readily detectable by plotting experimental deviates against corresponding normal probability deviates (Abrahams & Keve, 1971; Abrahams, 1997). De Camp (1973) suggested that interatomic distances can be used as chemical coordinates. Half-normal probability (HNP) plot analysis is used to:

(i) investigate the reliability of the s.u.s and

(ii) identify the systematic geometrical differences in two molecules.

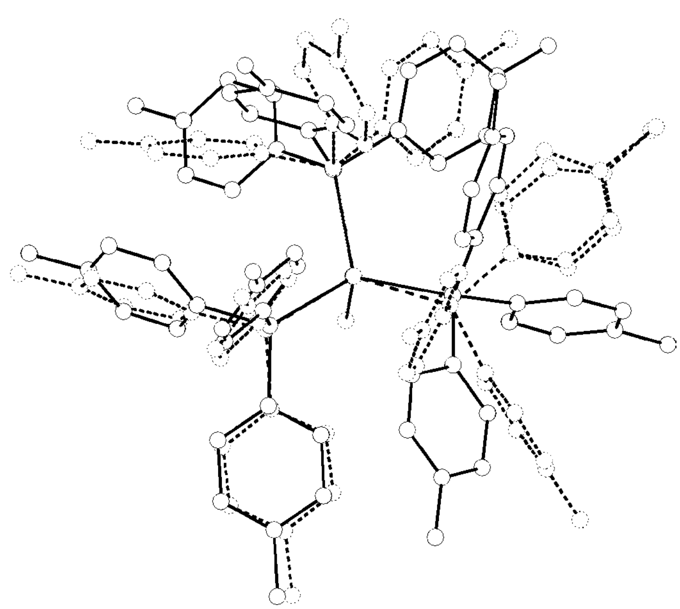

**Figure 3**
Overlay of polymorphs *a* (solid) and *b* (dotted).

[2] $D$—H$\cdots A$: C326—H326$\cdots$I1; $d(D$—H): 0.95 Å; $d(\text{H}\cdots A)$: 2.99 Å; $d(D\cdots A)$: 3.9335 (19) Å; $\angle(DHA)$: 171.9°.

Observed values of $\delta m_i$, calculated using (1), are plotted *versus* the $\alpha_i$ values expected for a half-normal distribution of errors. The expected values ($\alpha_i$) for normal and half-normal probability deviates were tabulated (Hamilton, 1974), but can also be derived from the *Tables of Normal Probability Functions* (National Bureau of Standards, 1953)

$$\delta m_i = \frac{\left|d(1)_i - d(2)_i\right|}{\left[\sigma^2 d(1)_i + \sigma^2 d(2)_i\right]^{1/2}}. \qquad (1)$$

The quantities $d(1)_i$ and $d(2)_i$ are interatomic distances for two different structures (1) and (2) with s.u.s $\sigma d(1)_i$ and $\sigma d(2)_i$, respectively. Two different comparisons can be made, the first using dependent distances – representing atoms separated by one, two or three formal bonds – and the second using independent distances. For 68 non-H atoms, 198 independent interatomic distances ($3n - 6$) completely describe the complex. To ensure a non-biased comparison only 198 dependent distances were used in the calculations. These distances represent the direct bond lengths (76; first order), bond angles (77; second order) and torsion angles (45; third-order distances) – excluding the minor component of the disordered *p*-tolyl group in polymorph *b*.

The dependent distances are used to identify interatomic distances that are significantly different for the compared

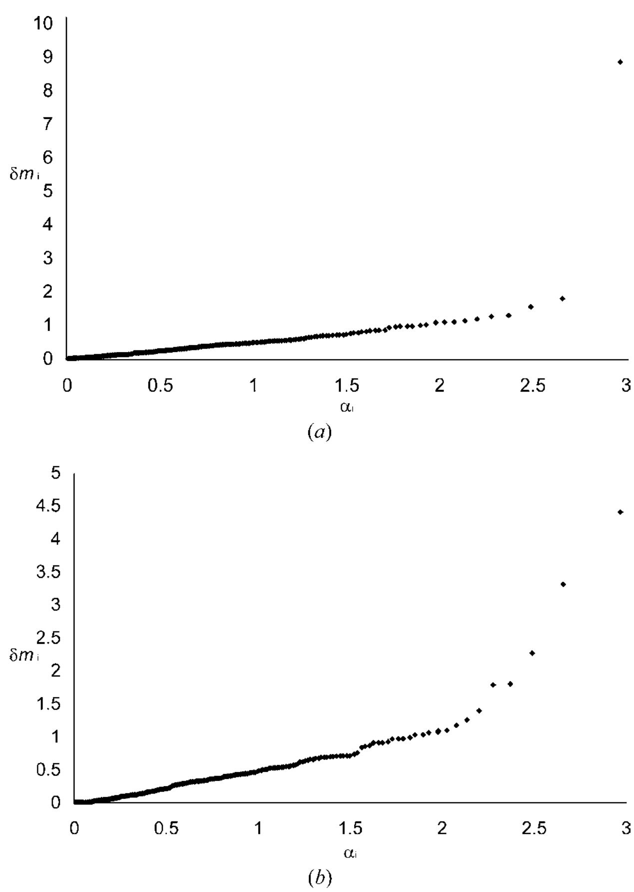


**Figure 4**
Half-normal probability plots with (*a*) 198 dependent and (*b*) independent distances for two crystals of two datasets of polymorph *b* at 293 K.

**Table 5**
Interatomic distances with the largest $\delta m_i$ for the two polymorphs *a* and *b*, ignoring the disordered *p*-tolyl group.

| Polymorph *b*, 293 K (Meijboom, 2007) *versus* 293 K (Zartilas *et al.*, 2007) | | | Polymorph *a versus* polymorph *b* | | |
|---|---|---|---|---|---|
| $\delta m_i$ | Distance | Order† | $\delta m_i$ | Distance | Order† |
| 2.20 | C221—C226 | First | 17.35 | I1—P2 | Second |
| 2.13 | I1—C221 | Third | 17.29 | I1—P3 | Second |
| 2.08 | Ag1—C322 | Third | 16.86 | I1—C331 | Third |
| 2.03 | Ag1—I1 | First | 12.65 | Ag1—C132 | Third |
| 1.98 | C322—C324 | Second | 10.99 | P1—P2 | Second |
| 1.93 | P1—C136 | Second | 9.82 | Ag1—C212 | Third |
| 1.90 | P3—C322 | Second | 9.13 | Ag1—C322 | Third |
| 1.85 | C126—C127 | Third | 7.21 | Ag1—C112 | Third |
| 1.83 | Ag1—P1 | First | 5.34 | Ag1—C122 | Third |
| 1.79 | C114—C115 | First | 5.08 | I1—P1 | Second |

† First-, second- and third-order number represents the closest distance between two atoms separated by one, two or three formal bonds.

molecules (Figs. 4*a* and 5*a*) and thus provide a quantitative companion for r.m.s. error calculations. The largest deviates ($\delta m_i$) for the dependent distances represent the largest geometric differences between the compared structures.

In contrast, the independent distances need to be analysed as a complete set. From the graph obtained by using independent distances, a slope and an intercept (Figs. 4*b* and 5*b*) can be obtained by linear regression. A linear plot with a slope of unity and a zero intercept indicates a correct match between the compared sets of distances and correctly estimated s.u.s. If the slope is larger (or smaller) than unity the s.u.s are underestimated (or overestimated). A non-linear plot, or a linear plot with a nonzero intercept, on the other hand, indicates systematic differences, which may be caused by either geometrical differences in the compared compounds or by systematic errors in the measurement procedure.

Figs. 4 and 5 show the half-normal probability plots for the current complex. Fig. 4(*a*) shows the dependent bond-distance comparison of the two datasets of polymorph *b* at 293 K, whereas Fig. 4(*b*) shows the independent bond distances for these datasets. Fig. 5(*a*) shows the comparison of dependent bond distances of polymorph *a* (at 100 K) with *b* (at 293 K; Meijboom, 2007), whereas Fig. 5(*b*) shows the independent comparison. In Table 5 the largest differences of bond lengths, ignoring the disordered groups, are given.

Analysis of the HNP of the dependent distances of polymorph *b* shows that the largest differences between the various determinations are in the disordered *p*-tolyl group (Fig. 4*a*). When excluding the disordered group, only a few relatively small structural deviates were observed between the three independent collections of polymorph **b**. In addition, the HNP of the independent distances of these collections (Fig. 4*b*) showed a straight line with an intercept of almost zero (−0.05), and a slope of less than unity (0.62) up to $\alpha_i$ = 1.8 indicating that the s.u.s are slightly overestimated.

In contrast, the HNP comparing polymorph *a* and polymorph *b* (at 293 K; Meijboom, 2007) shows large differences between the structures. It can be seen from Table 4 that the largest differences are in the geometry around the Ag atom.

All the second-order distances, representing the angles around the Ag atom are represented in Table 5 (*cf.* Table 2). In addition, the third-order distances, representing the torsion angles, between the Ag atom and the second C atom of the *p*-tolyl rings are represented in this table. These distances support the r.m.s. overlay (Fig. 3) that the major geometric differences between polymorph *a* and *b* are the geometry around the Ag atom and the rotation of the *p*-tolyl groups in the phosphines.

The HNP comparing the independent distances of polymorph *a* and polymorph *b* shows clearly a non-linear behaviour. This is an addititional indication of geometric differences between the two structures.

It was reported previously (Chandrasekhar & Bürgi, 1983) that the conformational changes of $PR_3$ groups in square-planar complexes of the general form $[XM(PR_3)_3]$ ($X$ = halide; $M$ = Rh, Pt; $R$ = Me, Et, $^i$Pr, Ph) show a strongly correlated behaviour. The behaviour was described as resembling a gearing motion of interlocking cogwheels. In the current complex it seems clear that the three phosphine groups behave synergistically. A small conformational change in one of the phosphines leads to increasingly larger changes in the other two phosphines.

The appearance of polymorphism of this complex might be attributed to solvent influence, which is $CH_3CN$ in polymorph *a*, and a 1:1 $MeOH/CH_3CN$ mix in the case of polymorph *b*.

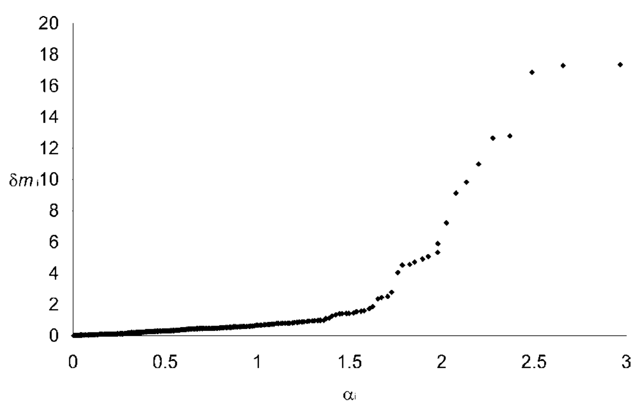


(*a*)

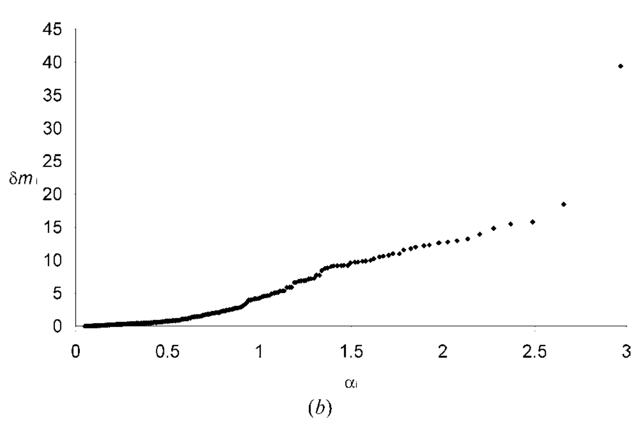


(*b*)

**Figure 5**
Half-normal probability plots with (*a*) 198 dependent and (*b*) independent distances for two crystals of polymorph *a* (100 K) and *b* (293 K).

Although the differences between the characteristics of these solvent systems might seem small, it should be realised that $[AgI(PPh_3)]_4$ crystallizes as a 'cubane' tetramer from $CHCl_3/Et_2O$ (Teo & Calabrese, 1976*a*) and as its 'step' analogue from $CH_2Cl_2/Et_2O$ (Teo & Calabrese, 1976*b*).

## 4. Conclusion

In conclusion, two polymorphs of $[AgI\{P(4-MeC_6H_4)_3\}_3]$ were analyzed and compared using r.m.s. overlay calculations and half-normal probability plot analysis. The space group of the current polymorph is monoclinic C2/*c* ($Z$ = 8), whereas the previously reported polymorph crystallizes in the triclinic space group $P\overline{1}$ ($Z$ = 2). The orientation of the *p*-tolyl moieties on the phosphine ligands is vastly different and constitutes a contributing factor in the difference between the two polymorphs. Additionally, the solvent of crystallization probably plays an influence in the polymorphic crystallization of silver complexes.

Financial assistance from the DST-NRF Centre of Excellence in Catalysis (c*change), the Research Fund of the University of the Free State, SASOL, THRIP, and the NRF is gratefully acknowledged. Part of this material is based on work supported by the South African National Research Foundation (SA NRF, GUN 2038915). Opinions, findings, conclusions or recommendations expressed in this material are those of the author and do not necessarily reflect the views of the NRF. Dr A. J. Muller is acknowledged for collection of the X-ray data. Professor Å Oskarsson (University of Lund) is thanked for help with the half-normal probability plots.

## References

Abrahams, S. C. (1997). *Acta Cryst.* A**53**, 673–675.
Abrahams, S. C. & Keve, E. T. (1971). *Acta Cryst.* A**27**, 157–165.
Allen, F. H. (2002). *Acta Cryst.* B**58**, 380–388.
Altomare, A., Burla, M. C., Camalli, M., Cascarano, G. L., Giacovazzo, C., Guagliardi, A., Moliterni, A. G. G., Polidori, G. & Spagna, R. (1999). *J. Appl. Cryst.* **32**, 115–119.
Bowmaker, G. A., Effendy, Kildea, J. D. & White, A. H. (1997). *Aust. J. Chem.* **50**, 577–586.
Brandenburg, K. & Putz, H. (2005). *DIAMOND*, Version 3.0c. Crystal Impact GbR, Bonn, Germany.
Bruker (2003). *COSMO*, Version 1.48. Bruker AXS Inc., Madison, Wisconsin, USA.
Bruker (2004*a*). *SAINT-PLUS*, Version 7.12. Bruker AXS Inc., Madison, Wisconsin, USA.
Bruker (2004*b*). *XPREP* and *SADABS*, Version 2004/1. Bruker AXS Inc., Madison, Wisconsin, USA.
Bruker (2005). *APEX*2, Version 1.0–27. Bruker AXS Inc., Madison, Wisconsin, USA.
Camalli, M. & Caruso, F. (1987). *Inorg. Chim. Acta*, **127**, 209–213.
Chandrasekhar, K. & Bürgi, H.-B. (1983). *J. Am. Chem. Soc.* **105**, 7081–7093.
De Camp, W. H. (1973). *Acta Cryst.* A**29**, 148–150.
De Gelder, R., Wehrens, R. & Hageman, J. A. (2001). *J. Comput. Chem.* **22**, 273–389.

Effendy, Kildea, J. D. & White, A. H. (1997). *Aust. J. Chem.* **50**, 587–604.

Engelhardt, L. M., Healy, P. C., Patrick, V. A. & White, A. H. (1987). *Aust. J. Chem.* **40**, 1873–1880.

Farrugia, L. J. (1999). *J. Appl. Cryst.* **32**, 837–838.

Hamilton, W. C. (1974). *International Tables for X-ray Crystallography*, Vol. IV, pp. 293–310. Birmingham: Kynoch Press.

Hibbs, D. E., Hursthouse, M. B., Malik, K. M. A., Beckett, M. A. & Jones, P. W. (1996). *Acta Cryst.* C**52**, 884–887.

Hypercube (2002). HyperChem Molecular Modeling System, Version 7.52. Hypercube Inc., Florida, USA.

Karfunkel, H. R., Rohde, B., Leusen, F. J. J., Gdanitz, R. J. & Rihs, G. (1993). *J. Comput. Chem.* **14**, 1125–1135.

Meijboom, R. (2006). *Acta Cryst.* E**62**, m2698–m2700.

Meijboom, R. (2007). *Acta Cryst.* E**63**, *m*78–*m*79.

Meijboom, R., Bowen, R. J. & Berners-Price, S. J. (2009). *Coord. Chem. Rev.* **253**, 325–342.

Meijboom, R. & Muller, A. (2006). *Acta Cryst.* E**62**, m3191–m3193.

Meijboom, R., Muller, A. & Roodt, A. (2006). *Acta Cryst.* E**62**, m2162–m2164.

Microsoft (2003). *Program for Spreadsheets and Graphics.* Microsoft Inc. USA.

National Bureau of Standards (1953). *Tables of Normal Probabilitity Functions.* Applied Mathematics Series, No. 23. US Government Printing Office, Washington, DC, USA.

Panattoni, C. & Frasson, E. (1963). *Gazz. Chim. Ital.* **93**, 601.

Pelizzi, C., Pelizzi, G. & Tarasconi, P. (1985). *J. Organomet. Chem.* **281**, 403–411.

Sheldrick, G. M. (2008). *Acta Cryst.* A**64**, 112–122.

Spek, A. L. (1990). *Acta Cryst.* A**46**, C34.

Teo, B.-K. & Calabrese, J. C. (1976*a*). *Inorg. Chem.* **15**, 2467–2474.

Teo, B.-K. & Calabrese, J. C. (1976*b*). *Inorg. Chem.* **15**, 2474–2486.

Venter, G. J. S., Meijboom, R. & Roodt, A. (2006). *Acta Cryst.* E**62**, m3453–m3455.

Venter, G. J. S., Meijboom, R. & Roodt, A. (2007). *Acta Cryst.* E**63**, m3076–m3077.

Venter, G. J. S., Roodt, A. & Meijboom, R. (2008). Unpublished results.

Willighagen, E. L., Wehrens, R., Verwer, P., de Gelder, R. & Buydens, L. M. C. (2005). *Acta Cryst.* B**61**, 29–36.

Zartilas, S., Hadjikakou, S. K., Hadjiliadis, N., Kourkoumelis, N., Kyros, L., Kubicki, M., Baril, M., Butler, I. S., Karkabounas, S. & Balzarini, J. (2007). *Inorg. Chim. Acta*, doi:10.1016/j.ica.2007.07.034.